Narrow Size-Distribution Poly(methyl methacrylate) Nanoparticles Made by Semicontinuous Heterophase Polymerization

J. Aguilar,[1] M. Rabelero,[1] S. M. Nuño-Donlucas,[1] E. Mendizábal,[1] A. Martínez-Richa,[2] R. G. López,[3] M. Arellano,[1] J. E. Puig[1]

[1]*Departamento de Ingeniería Química y de Química, Universidad de Guadalajara, Boul. M. García Barragán No. 1451, Guadalajara, Jal. 44430, México*
[2]*Departamento de Química, Universidad de Guanajuato, Noria Alta s/n, Guanajuato, Gto. 36000, México*
[3]*Centro de Investigación en Química Aplicada, Boul. Ing. E. Reyna No. 140, Saltillo, Coah. 25253, México*

Received 24 December 2009; accepted 31 May 2010
DOI 10.1002/app.32886
Published online 23 August 2010 in Wiley Online Library (wileyonlinelibrary.com).

ABSTRACT: The effect of surfactant (sodium dodecyl sulfate) concentration on particle size, molar masses, glass transition, and tacticity of poly(methyl methacrylate) (PMMA) nanoparticles synthesized by semicontinuous heterophase polymerization under monomer-starved condition at constant monomer feeding rate is reported. Starved conditions are confirmed by the low amount of residual monomer throughout the reaction and by the fact that the instantaneous polymerization rate is similar to the feeding rate of monomer. Under these conditions, polymer particles in the nanometer range (20–30 nm) were obtained with narrow size distribution ($1.07 < D_w/D_n < 1.18$), depending of surfactant concentration. Final particle size diminishes as the surfactant concentration is increased. Glass transition temperatures and syndiotactic content (54%–59%) of the produced polymers are substantially higher than those reported for commercial and bulk-made PMMA. Molar masses are much lower than those expected from termination by chain transfer to monomer, which is the typical termination mechanism in 0–1 emulsion and microemulsion polymerization of this monomer.
 J Appl Polym Sci 119: 1827–1834, 2011

Key words: radical polymerization; syndiotactic; particle size distribution; nanotechnology

INTRODUCTION

Microemulsion polymerization is a novel process that allows the synthesis of high molar mass ultrafine polymer particles with fast reaction rates in a routinely fashion.[1–5] Even though it is easier to achieve much smaller particle sizes than its counterpart emulsion process, the large amounts of surfactant used to produce relatively small amount of polymer particles limit this process for industrial scaling.[2,5] However, by semicontinuous addition of monomer or by diffusion-controlled addition of monomer from a neat monomer phase or from a Windsor II-type microemulsion, the amount of surfactant required to produce larger amounts of polymer particles (20%–35%) can be considerably reduced.[6–10]

Correspondence to: M. Arellano (marellan@cencar.udg.mx or marellan22@gmail.com).

Contract grant sponsor: Mexican Council of Science and Technology (CONACYT); contract grant number: CB-2007-82437.

Polymerization in one- and two-dimension confinement of vinyl monomers can give more highly isotatic or syndiotactic polymers (depending on monomer) than those in bulk or solution polymerization.[11–16] Likewise, three-dimension confinement of the monomer in the small volume of a microemulsion droplet should also influence the microstructure of the polymer formed therein, because one or few polymer chains per particle are produced in this process. In fact, it has been reported elsewhere that the microemulsion polymerization of methyl methacrylate (MMA) yields higher syndiotactic polymer than those made by bulk polymerization.[17–21] Others have also reported higher syndiotacticity in a variety of poly(alkyl methacrylates) produced by a modified microemulsion polymerization process.[22,23] However, tacticity for poly(methyl methacrylate) (PMMA) depends also upon temperature of the radical polymerization, and the syndiotacticity of the PMMA generally increases as the polymerization temperature diminishes.[18,24,25]

Recently, another semicontinuous polymerization method under monomer-starved conditions was reported to produce polymer nanoparticles with narrow size distribution and smaller molar masses than those obtained by semicontinuous emulsion and

microemulsion processes of similar monomers.[26–29] In this process, named by us as semicontinuous heterophase polymerization, neat monomer is added semicontinuously at controlled feeding rate to achieve monomer-starved conditions over a monomer-free aqueous solution of surfactant and initiator at the adequate temperature; clearly, no emulsified monomer droplets should be present in the system. In particular, it was shown that concentrated latex containing narrow size distribution polymer nanoparticles (20–30 nm with a size distribution width smaller than 1.05) could be produced, with average particle diameters and average molar masses that decrease with decreasing monomer-feeding rate.[29]

The issue here is whether the semicontinuous heterophase polymerization of MMA under monomer-starved conditions can also increase the amount of syndiotactic sequences in the polymer chain, with the advantage over microemulsion polymerization that much smaller amounts of surfactant are needed to yield particles in the nanometer range.

In this article, we examine the effects of varying surfactant concentration at a fixed monomer addition rate (such as to give monomer-starved conditions) on particle size, particle size distribution (PSD), molar masses, glass transition temperature, and syndiotacticity of PMMA synthesized by the semicontinuous heterophase polymerization.

EXPERIMENTAL

MMA (99% pure from Aldrich) was distilled under reduced pressure and stored at 4°C. Sodium dodecyl sulfate [SDS (98% pure from TCI America)] and potassium persulfate [KPS (99% pure from Aldrich)] were used as received. De-ionized and triple-distilled water was used.

Polymerizations were carried out in a 250-mL jacketed glass reactor equipped with a reflux condenser and inlets for nitrogen, monomer feed, sampling, and mechanical agitation. Initially, 70 g of aqueous SDS solution (at various SDS concentrations) containing 0.235 g KPS was loaded in the reactor, bubbled with nitrogen for 1 h, and heated to the reaction temperature (50°C), before initiating monomer addition. Then, the monomer was fed at a rate of 0.15 g/min using a dosing pump (Hel) equipped with a balance to control the rate of addition. In all runs, similar amounts of MMA ($\sim$ 23.5 g) were added. After the monomer addition was completed, the reaction was allowed to proceed for another 2 h. Samples were withdrawn at given times to determine the conversion gravimetrically and for measuring particle size, glass transition temperature, tacticity, and molar mass distribution. Polymer was precipitated from the withdrawn samples by adding methanol (Bassel, reactive grade), recovered by filtration and purified. Because the decomposition rate of KPS is pH-sensitive, pH was monitored during the reaction with an Orion 720A pH-meter, yielding values from 7.4 at the beginning of the reaction down to 6.4 at the end. In this pH range, the decomposition rate of KPS is not affected.[30]

z-Average particle size (Dp_z) as a function of reaction time was measured at 25°C by quasi-elastic light scattering (QLS) in a Malvern Zetasizer ZS90 apparatus. The particle size standard operating procedure subroutine was used to estimate the PSD. To eliminate multiple scattering and to measure the monomer-free average particle size, lattices were diluted with water up to 200 times.

Particle size and size distribution at the end of the polymerization were determined in a JEOL 1010 electron transmission microscope. The procedure was to dilute 20-times one drop of latex with water and deposited a drop of this dilution on a cooper grid; then, a drop of a 2 wt % phosphotungstic acid aqueous solution was added over the grid, which was allowed to dry overnight. At least 400 particles were measured from the micrographs to obtain the histograms and the D_w/D_n [particle size polydispersity index (PDI)], being D_w and D_n the weight- and number-average diameters, respectively, which were calculated by the following formulae:

$$D_n = \frac{\sum_i n_i D_i}{\sum_i n_i} = \frac{\sum n_i D_i}{n} \quad (1)$$

$$D_w = \frac{\sum_i n_i D_i^4}{\sum_i n_i D_i^3} \quad (2)$$

where n_i are the number of particles of size D_i, and n is the total number of measured particles.

Average molar masses were measured in a LC-30 Perkin–Elmer gel permeation chromatograph using tetrahydrofuran (THF) as the mobile phase. The calibration was made with polystyrene standards.

Solution ^{1}H and ^{13}C-NMR spectra of PMMA were recorded at room temperature in a Varian Unity Plus 300 NMR spectrometer, using chloroform-*d* ($CDCl_3$) as solvent. Spectra were referred to the tetramethylsilane signal. The tacticity of the samples was determined using the integrated ratios of the syndiotactic (rr), isotactic (mm), and heterotactic (mr) triad signal of α-methyl protons, as described elsewhere.[21,31]

Glass transition temperatures were measured in a Q100 modulated scanning calorimeter from TA Instruments calibrated with indium for temperature and sapphire for the modulation frequency. Measurements were performed at a heating rate of 3°C/min up to 150°C with a modulation frequency of 1/60 s^{-1} and a modulation amplitude of ±1°C using nitrogen purge gas flow of 50 mL/min. After the

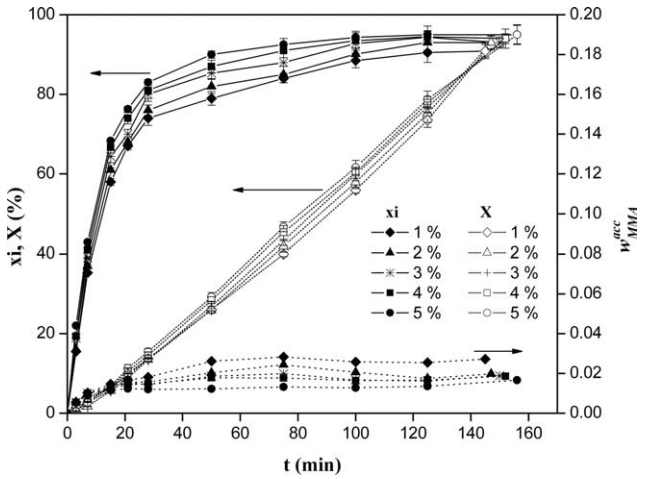

Figure 1 Evolution with time of instantaneous, x_i (——) and global, X (– – –) conversions and residual monomer weight fraction (w^{acc}_{MMA}) for the polymerization of MMA at different surfactant concentrations.

first heating scan, samples were quenched to 25°C at 200°C/min, and a second scan was carried out at equal heating rate (3°C/min). The glass transition temperatures were evaluated from the second scan by analyzing the reversible heat flow signal using the criteria of half-height.

RESULTS AND DISCUSSION

The initial transparent surfactant solution becomes bluish and increasingly opaque and more viscous with the progress of monomer addition and reaction time. The lattices have shown no sign of coagulation and have remained stable for over six months of storage at room temperature.

Figure 1 depicts the instantaneous (x_i) and the global (X) conversions as well as the residual (or non-reacted) monomer weight fraction (w^{acc}_{MMA}) versus time t for the various SDS concentrations (C_{SDS}) used in the process carried out at 50°C. The instantaneous conversion [$x_i(t)$] is the fraction of added monomer up to time t that has changed into polymer, whereas the global conversion [$X(t)$] is the ratio of monomer added that has reacted into polymer at time t divided by the total amount of monomer added in the process. Both conversions were calculated from gravimetric measurements of samples taken at given times and mass balances. The weight fraction of residual monomer (w^{acc}_{MMA}) is defined as the weight of nonreacted monomer divided by total weight of reacting mixture at given time. Figure 1 reveals that x_i increases rapidly and reaches high values (ca. 80%) at ca. 30 min, regardless of C_{SDS}. After this initial period, x_i increases more slowly and remains high throughout the reaction. Moreover, x_i increases with increasing C_{SDS} during the whole semicontinuous operation. The w^{acc}_{MMA} is small and diminishes with increasing C_{SDS} as expected because there is more surfactant available to stabilize newly formed particles. The small and nearly constant values of w^{acc}_{MMA} achieved throughout most of the reaction suggest that monomer-starved conditions were achieved for all the surfactant concentrations studied here.

The comparison of the instantaneous polymerization rate (R_P) and the monomer-feeding rate (R_a) indicates whether monomer-starved conditions are achieved because for semicontinuous processes under monomer-starved conditions, $R_p \cong \phi_p R_a$, where ϕ_P is the volume fraction of polymer in the monomer-swollen particles.[32] Because for most semicontinuous emulsion polymerizations operating at steady state under monomer starving conditions, $\phi_P > 0.9$, then a rule of thumb for monomer-starved conditions is that $R_P \approx R_a$.[33] In fact, Sajjadi reported that $R_P \approx R_a$ for semicontinuous emulsion polymerization of butyl acrylate and vinyl acetate under monomer-starved conditions.[28] Figure 2 depicts R_P/R_a as a function of time; R_P was estimated numerically from the slope of the curve of x_i versus t (Fig. 1). This figure reveals that this ratio rises rapidly with time and achieves a steady state value after 20–25 min, regardless of the C_{SDS}. In the plateau region, this ratio increases slightly with increasing C_{SDS}, as expected from the instantaneous conversion curves (Fig. 1) and achieves values of about 0.95–0.97, demonstrating that monomer-starved conditions were attained at all SDS concentration examined.

Figure 3 depicts QLS-measured z-average particle size (Dp_z) as a function of global conversion for the

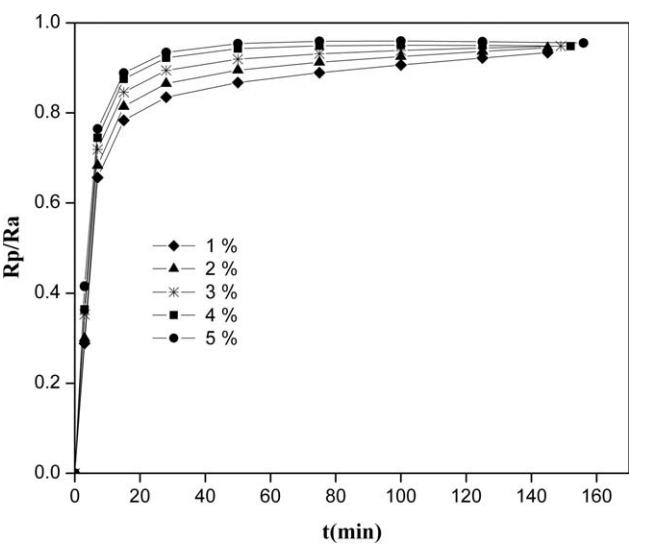

Figure 2 Ratio of the instantaneous polymerization and the monomer addition rates (R_p/R_a) as a function of time for the polymerization of MMA at different SDS concentrations.

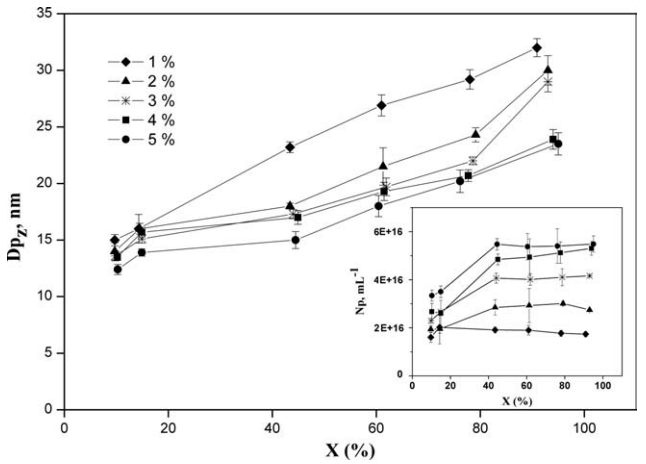

Figure 3 z-Average particle size (Dp_z), measured by QLS, and average number density of particle (N_p) versus global conversion for the polymerization of MMA at different surfactant concentrations.

different SDS concentrations used in the reactions. Dp_z increases systematically with increasing conversion (and solid content) and decreasing SDS concentration. It is remarkable that the final Dp_z, which ranges from 23 to 32 nm, is similar to those typically obtained in batch and semicontinuous microemulsion polymerization processes.[1–10,17–20,22–23] Nevertheless, the lowest amount of surfactant used here (1 wt %) is substantially smaller than those in batch and semicontinuous microemulsion polymerization processes and still similar particle sizes are obtained. Moreover, the ratio of polymer-to-surfactant is larger in our process than the ones obtained in microemulsion polymerization, even for the semicontinuous ones.[10–12] The evolution of the average number density of particles (N_P) as a function of global conversion is shown in insert of Figure 3. N_P was estimated with the assumptions that particles are spherical and all have the same size and using the following formula:

$$N_{\mathrm{p}}(t) = \frac{6M(t)x_i}{\pi D_{\mathrm{p}}^3(t)\rho_{\mathrm{Pol}}} \tag{3}$$

here, $M(t)$ is the weight of monomer per milliliter of latex added at time t, $D_P(t)$ is the particle size at time t and ρ_{Pol} is the density of PMMA, which was taken as equal as that of bulk PMMA. The inset shows that N_P increases rapidly at early stages of the reaction but, at $\sim$ 40% conversion, growth in the number of particles slows down and at higher conversions, there is a small increase in N_P.

Figure 4 depicts a representative TEM micrograph, where spherical particles in the nanometer range with narrow size distribution can be observed. Figure 5 shows PSDs, determined by QLS (continuous line), and the histograms, determined by TEM, of the particles obtained using 3 and 5 wt % SDS. Both the PSDs and the histograms

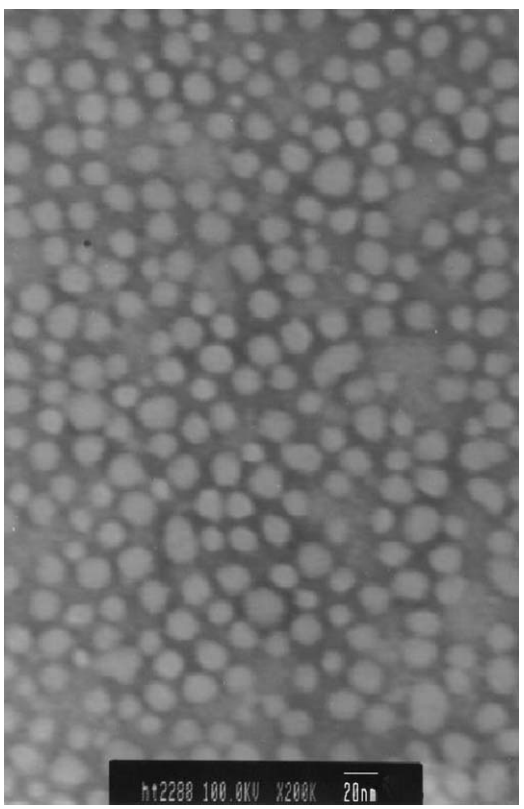

Figure 4 TEM micrograph of final latex prepared by polymerization of MMA using 5% initial surfactant concentration at 50°C.

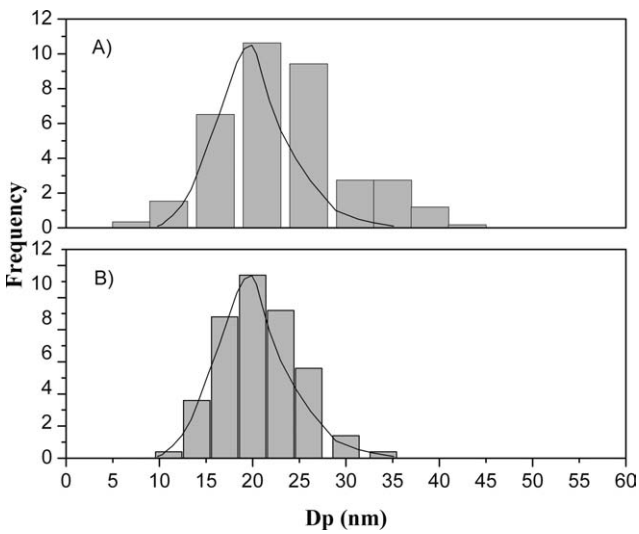

Figure 5 Size distributions obtained from TEM photographs (histograms) and QLS-measured size distribution (continuous lines) of final latex samples prepared by polymerization of MMA at different surfactant concentrations: (A) 3 wt % and (B) 5 wt %.

TABLE I
Final Average Particle Size and PDI[a], Number-Average Particle Size and D_w/D_n[b], Surface Coverage Ratio, Number-Average Molar Masses and Molar Mass Polydispersity for the Different SDS Concentrations

% SDS	D_z[a] (nm)	PDI[a]	D_n[b] (nm)	D_w/D_n[b]	r	M_n (10^5 Da)	M_w/M_n
1	32	1.18	35	1.21	0.19	2	2.2
2	30	1.16	32	1.19	0.38	2.1	2.1
3	29	1.13	31	1.16	0.58	2	2.3
4	24	1.11	27	1.11	0.67	2.4	2.1
5	23	1.09	24	1.07	0.75	1.1	2.4

[a] Determined by QLS.
[b] Determined by TEM.

nearly coincide, indicating that noninvasive QLS can be used instead of TEM, which may introduce artifacts due to sample handling, drying of sample on the grid, and electron beam damage. Table I reports final QLS particle size PDI and D_w/D_n obtained from the TEM histograms for the different SDS concentrations used in this study. An important feature of the process studied here is that narrow PSDs are obtained. This may be counterintuitive because a wider size distribution should be expected when nucleation is continuous during the whole reaction. For semicontinuous polymerization under monomer-starved conditions, the growth of the particles formed at low conversions is restricted by the very low monomer concentration within the particles and hence, formation of new particles predominates over the swelling and growing of the existing ones due to monomer diffusion. Under the experimental conditions used in this work, the formation of new particles after $\sim$ 40% conversion is quite small (see inset in Fig. 3) as a consequence of the small amount of surfactant used, which explains the rather narrow PSDs at the end of the reactions. In fact, after all available surfactant is adsorbed on the surface of the existing particles, which takes place at $\sim$ 40% conversion as described below, the monomer added afterwards preferentially diffuse into the existing particles to continue the reaction. This causes the increase in size due to formation of polymer chains within the particles.

An important feature of the process is that, even at the lowest SDS concentration used here (1 wt %), the size distribution is relative narrow (1.18) compared with those typically obtained in emulsion and microemulsion processes.[2,8,10–12,34] Moreover, as demonstrated elsewhere, narrower size distributions ($D_w/D_n < 1.1$) can be obtained at a fixed surfactant concentration by diminishing monomer addition rate by semicontinuous heterophase polymerization; however, fairly large amounts of surfactant (5 wt %) were used.[29] Here, we showed that similar results could be obtained with surfactant concentrations as low as 1 wt % yielding stable latexes with $\sim$ 25 wt % solid content.

The surface coverage ratio, r, defined as the total surface coverage by the available surfactant (total surfactant concentration – cmc) divided by the total surface area of the particles, can be estimated from particle size, N_P, the knowledge of the value of the molecular surface coverage (a_s) for SDS,[35] and by assuming that all particles have the same size, equal to the average-number diameter (D_n) determined by TEM. The values of r for the lattices obtained at the end of polymerizations are reported in Table I. At the end of polymerization, $r < 1$ for all cases and it decreases systematically as the SDS concentration diminishes. Values of r smaller than one were achieved at conversions ($\sim$ 40%) at which N_P increase diminishes substantially (see inset in Fig. 3). Similar low surface coverage ratios were reported by Sajjadi for poly(vinyl acetate) particles produced by monomer-starved semicontinuous emulsion polymerization.[28]

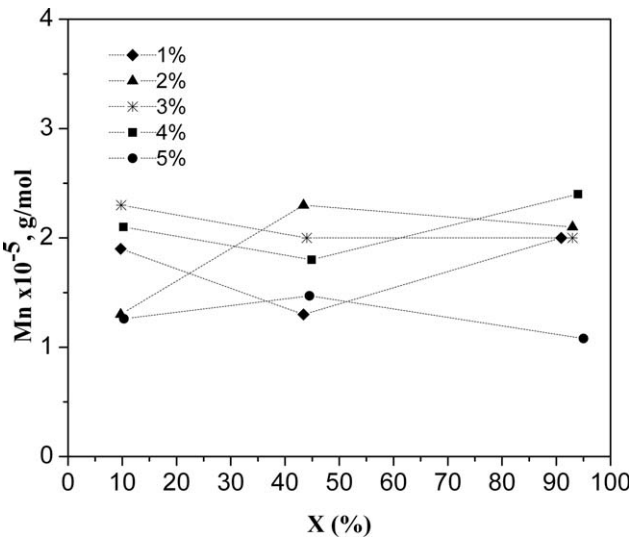

Figure 6 Number-average molar masses of PMMA as a function of global conversion for the different SDS concentrations used.

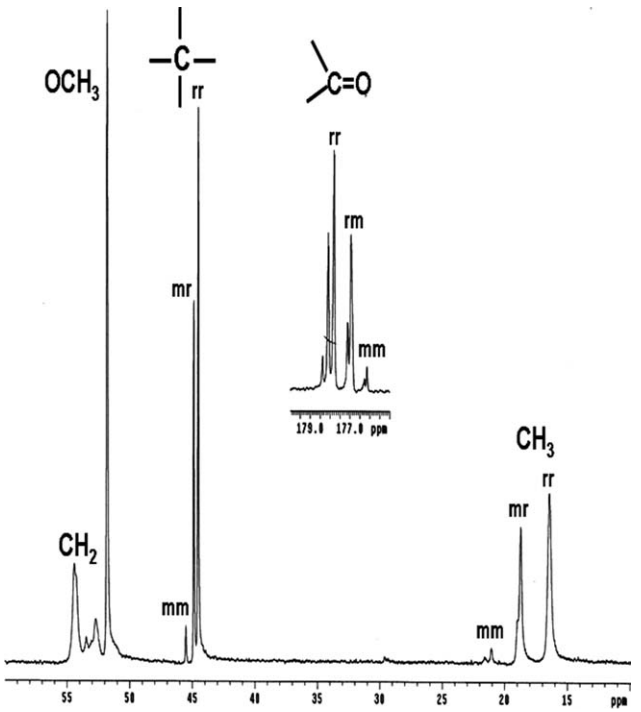

Figure 7 75-MHz ^{13}C-NMR spectrum of the PMMA obtained at the end of the semicontinuous heterophase polymerization using 2 wt % SDS.

Figure 6 displays the number-average molar masses (M_n) versus conversion for the different SDS concentrations used during the polymerization process. This figure reveals that (i) molar masses are practically independent of the SDS concentration used during the polymerization, (ii) molar masses remain constant all through the reaction, and (iii) number-average molar masses are one order of magnitude smaller than those expected from chain transfer to monomer, which is the expected termination mechanism for PMMA synthesized by batch microemulsion polymerization.[36]

Because monomer concentration in the particles is extremely low, chain growth is slow and before the probability for chain transfer to monomer occurs (this is because in the average, the addition of 30,000 monomer units is required to produce the event of chain transfer to monomer),[36] a radical can enter the particle causing chain growth termination by mutual radical annihilation, yielding as a result, small number-average molar masses. The PDI (M_w/M_n), reported in Table I, does not vary with surfactant concentration and its value is similar to that obtained by termination due to disproportion (2.0), which can be explained because although chain growth termination is by coupling, one of the radicals is very small.

Figure 7 displays a representative ^{13}C-NMR spectrum of the PMMA obtained at the end of the polymerization. In this spectrum, the syndiotactic (rr), heterotactic (*mr*), and isotactic (*mm*) triad peaks for the α-methyl, quaternary, and carbonyl carbons can be distinguished. Signals for methylene and methoxy groups are not sensitive to tacticity. As peak areas recorded in ^{1}H-NMR spectrum (not shown) are more quantitative,[21,31] the peaks for the α-methyl protons at 0.85, 1.02, and 1.20 ppm were used to determine syndiotacticity, heterotacticity and isotacticity in the PMMA produced here. The analysis of the integrated ratios of these triads reveals that the polymers are richer in syndiotactic content (54–59%, see Table II), and larger than those reported for bulk-made and commercial PMMA (Plexiglas) (43–48%).[37–39] On the other hand, Pilcher and Ford[18] reported even higher syndiotacticity in their samples made by batch microemulsion polymerization; however, it is noteworthy that the molar masses reported by these authors are almost an order of magnitude larger than the ones obtained here and by Jiang et al.[19] Our results are consistent with the stereoregularity reported for PMMA by other authors at similar polymerization temperatures but with advantage that smaller surfactant concentration and larger polymer solids are obtained here.[18,19]

For PMMA, the penpenultimate as well as the penultimate repeat unit of a growing chain in solution influence the configuration of the new stereocenter.[40] Also, the conformation of a polymer chain in a reacting nanoparticle is more compact than its usual random coil conformation in bulk. As a result, more gauche conformations near the end of a growing chain (where the penpenultimate and the penultimate units are located), especially near the surface of the particle, may influence the probability of forming meso and racemic diads. Therefore, the tacticity of PMMA formed in microemulsion and heterophase polymerizations might differ from that formed in bulk polymerization. It is noteworthy that the syndiotacticity of our samples is similar to that reported for PMMA synthesized by semicontinuous (or modified) microemulsion polymerization,[19,20] but smaller than

TABLE II
Glass Transition Temperature and Tacticity of the PMMA Obtained by Heterophase Polymerization at 50°C Using Different SDS Concentrations

% SDS	T_g[a] (°C)	T_g[b] (°C)	rr (%)	mr (%)	mm (%)
1	129	120	57	35	8
2	129	122	57	35	8
3	130	124	56	36	8
4	130	124	54	34	12
5	129	123	59	34	7

[a] First scan.
[b] Second scan.

the ones for PMMA made by batch microemulsion polymerization.[18] However, the molar masses of our PMMA samples (see Table I) and those in Refs. 19 and 20 are nearly one-order of magnitude smaller than the ones made by batch microemulsion polymerization,[18] yielding more chains per particle in the former processes compared with those in the later one. Hence, the PMMA chains made by batch microemulsion polymerization have a more compact state than the ones synthesized here or by the modified microemulsion polymerization. As a result, the restricted volume effect weakens resulting in polymers with lower syndiotacticity. In fact, Jiang et al. demonstrated that upon addition of a chain transfer agent to reduce PMMA molar masses in the nanoparticles, the syndiotacticity dropped to values similar to those of commercial PMMA.[19]

Table II also reports the glass transition temperatures (obtained at the first and second scans) of the polymers produced at the end of the reactions, for the different surfactant concentrations used here. The glass transition temperatures obtained here are consistently larger than that of PMMA made by bulk polymerization (T_g = 103°C)[41] and the higher value reported for the commercial PMMA (T_g = 115°C).[42] Moreover, they are similar to the ones produced by batch and modified microemulsion polymerization.[18–20] Clearly, the higher T_g's of our polymers and those made by microemulsion polymerization[18–20] are related to the higher polymer syndiotacticity; as a matter of fact, the reported glass transition temperature range for pure syndiotactic PMMA between 127°C and 141°C, those for pure atactic one range from 105°C to 107°C, and those for the pure isotatic polymer are only from 38°C to 52°C.[41] Tang et al. also reported higher syndiotacticity and larger T_gs for several poly(alkyl methacrylates) contained in nanoparticles made by modified microemulsion polymerization compared with those of bulk- or solution-made ones.[20]

CONCLUSIONS

Here, we reported a simple method to produce syndiotactic-rich PMMA nanoparticles of narrow size distributions. Latex with high solid contents can be produced with surfactant concentrations similar to those used in emulsion polymerization. The effect of surfactant concentration on particles size, molar masses, and polymer characteristics is reported here. Moreover, and in contrast to the (batch and modified) microemulsion polymerizations, the method used here is simpler, requires less amounts of surfactant, yields larger solid contents and produces nanoparticles of narrow size distributions and modified stereoregularity in a routinely fashion, which are difficult to achieved by either emulsion or microemulsion polymerization.

J. Aguilar thanks CONACYT for scholarship. All the authors are indebted to QB Karla Barrera-Rivera (UG) for obtaining NMR spectra.

References

1. Full, A. P.; Puig, J. E.; Gron, L. U.; Kaler, E. W.; Minter, J. R.; Mourey, T. H.; Texter, J. Macromolecules 1992, 25, 5157.
2. Puig, J. E. In The Polymeric Materials Encyclopedia. Synthesis, Properties and Applications, Vol. 6; Salamone, J. C., Ed.; CRC Press: Boca Ratón, 1996.
3. Puig, J. E. Rev Mex Fis 1999, 45(S1), 18.
4. de Vries, R.; Co, C. C.; Kaler, E. W. Macromolecules 2001, 34, 3233.
5. Co, C. C.; de Vries, R.; Kaler, E. W. In Reactions and Synthesis in Surfactant Systems, Surfactant Science Series Vol. 100; Texter, J, Ed.; Marcel Dekker: New York, 2001; Chapter 22.
6. Rabelero, M.; Zacarías, M.; Mendizábal, E.; Puig, J. E. Polym Bull 1997, 8, 695.
7. Xu, X. J.; Chew, C. H.; Siow, K. S.; Wong, M. K.; Gan, L. M. Langmuir 1999, 15, 8067.
8. Ming, W. H.; Jones, F. N.; Fu, S. Macromolecular Chem Phys 1998, 199, 1075.
9. Ming, W. H.; Jones, F. S.; Fu, K. S. Polym Bull 1998, 40, 749.
10. Sosa, N.; Peralta, R. D.; López, R. G.; Ramos, L. F.; Katime, I.; Cesteros, C.; Mendizábal, E.; Puig, J. E. Polymer 2001, 42, 6923.
11. Blumstein, A. Adv Macromol Chem 1970, 2, 123.
12. Tsutsumi, H.; Okanishi, K.; Miyata, M.; Takemoto, K. J Polym Sci Part A: Polym Chem 1990, 28, 1527.
13. Minagawa, M.; Yamada, H.; Yamaguchi, K.; Yoshi, F. Macromolecules 1992, 25, 503.
14. Allcock, H. R.; Silverberg, E. N.; Dudley, G. K. Macromolecules 1994, 27, 1033.
15. Regen, S. L.; Shin, J.-S.; Yamaguchi, K. J Am Chem Soc 1984, 106, 2446.
16. Fukuda, H.; Diem, T.; Stefeley, J.; Kezdy, F. J.; Regen, S. L. J Am Chem Soc 1986, 108, 2321.
17. Roy, S.; Devi, S. Polymer 1997, 38, 3325.
18. Pilcher, S. C.; Ford, W. T. Macromolecules 1988, 31, 3454.
19. Jiang, W.; Yang, W. L.; Zeng, X. B.; Fu, S. K. J Polym Sci Part A: Polym Chem 2004, 42, 733.
20. Tang, R.; Yang, W.; Zha, L.; Fu, S. J Macromol Sci Part A: Pure Appl Chem 2008, 45, 345.
21. Martínez-Richa, A.; Cauich-Rodríguez, J. V.; Vera-Graziano, R. Polym Prepr (Am Chem Soc Div Polym Chem) 2000, 82, 17.
22. Tang, R.; Yang, W. L.; Wang, C. C.; Fu, S. K. J Macromol Sci Part A: Pure Appl Chem 2005, 42, 291.
23. Tang, R.; Xue, Y.; Zha, L.; Fu, S. J Macromol Sci Part A: Pure Appl Chem 2007, 44, 569.
24. Isobe, Y.; Yamada, K.; Nakano, T.; Okamoto, Y. Macromolecules 1999, 32, 5979.
25. Satoh, K.; Kamigaito, M. Chem Rev 2009, 109, 5120.
26. Sajjadi, S. J Polym Sci Part A: Polym Chem 2001, 39, 3940.
27. Sajjadi, S.; Yianneski, M. Polym Reaction Eng 2003, 11, 715.
28. Sajjadi, S. Langmuir 2007, 23, 1018.
29. Ledezma, R.; Treviño, M. E.; Elizalde, L. E.; Pérez-Carrillo, L. A.; Mendizábal, E.; Puig, J. E.; López, R. G. J Polym Sci Part A: Polym Chem 2007, 45, 1463.
30. Santos, A. M.; Vindevoghel, P. H.; Graillat, C.; Guyot, A.; Guillot, J. J Polym Sci Part A: Polym Chem 1996, 34, 1271.
31. Hatada, K.; Ora, K.; Yuki, H. J Polym Sci Part A2: Polym Phys 1967, 5, 225.

32. Wessling, R. A. J Appl Polym Sci 1968, 1, 309.
33. Lovell, P. A. In Emulsion Polymerization and Emulsion Polymers; Lovell, P. A., El-Aasser, M. A., Eds.; Wiley: New York, 1997, Chapter 7.
34. Gilbert, R. G. Emulsion Polymerization. A Mechanistic Approach; Academic Press: New York, 2004.
35. Matijevic, E.; Pathica, B. A. Trans Faraday Soc 1958, 54, 1382.
36. Rodríguez-Guadarrama, L. A.; Mendizábal, E.; Puig, J. E.; Kaler, E. W. J Appl Polym Sci 1993, 48, 775.
37. Thompson, E. V. J Polym Sci Part A2: Polym Phys 1966, 4, 199.
38. Vandeweerdt, P.; Berghmnas, H.; Tervoot, Y. Macromolecules 1991, 24, 3547.
39. Hub, C.; Harton, S. E.; Huint, M. A.; Fink, R.; Ade, H. J Polym Sci Part B: Polym Phys 2007, 45, 2270.
40. Moad, G.; Soloman, D. H.; Spurling, T. H.; Johns, S. T.; Willing, R. I. Aust J Chem 1986, 39, 43.
41. Andrews, R. J.; Grulke, E. A. In Polymer Handbook; Brandrup, J., Immergut, J., Grulke, E.A., Eds.; Wiley: New York, 1998; pp VI/193–278.
42. Faivre, A.; David, L.; Vassoille, R.; Vigier, G.; Etienne, S.; Geissler, E. Macromolecules 1996, 29, 8387.